

Optimum Noncoherent Detection of Constant-Envelope Signals using Received Signal Magnitudes — Energy Detection and Amplitude Detection

Mu Jia*, Junting Chen*, Ying-Chang Liang[†] and Pooi-Yuen Kam*

* School of Science and Engineering and Shenzhen Future Network of Intelligence Institute (FNii-Shenzhen)
The Chinese University of Hong Kong, Shenzhen, Guangdong 518172, China,

[†] Center for Intelligent Networking and Communications (CINC)

University of Electronic Science and Technology of China (UESTC), Chengdu 611731, China.

Abstract—Constant-envelope signals are widely employed in wireless communication systems due to their hardware-friendly design, energy efficiency, and enhanced reliability. However, detecting these signals reliably using simple, power-efficient receivers remains a critical challenge. While coherent detection methods generally offer superior performance, they require complex frequency synchronization, which increases receiver complexity and power consumption. In contrast, noncoherent detection is inherently simpler since it avoids frequency synchronization. However, traditional noncoherent detection approaches still rely on In-phase and Quadrature-phase (IQ) demodulators to extract the noisy received signal magnitudes, and assume the energy detector as the test statistic according to the IQ structure, without rigorous theoretical justification. Motivated by the practical need for robust and low-complexity detection, this paper proposes a comprehensive framework for optimal signal detection using a simple bandpass-filter envelope-detector (BFED) in conjunction with a Bayesian approach and the generalized likelihood ratio test (GLRT) under unknown amplitude conditions. By leveraging approximations of the modified Bessel functions, we derive two distinct regimes of the optimal detector. In the low SNR regime, we rigorously prove that the energy detector emerges as the Bayesian-optimal solution, thereby establishing its theoretical validity for the first time. In the high SNR regime, we derive a novel amplitude-based detector that directly compares the estimated amplitude against the noise standard deviation, leading to a simple yet optimal detection strategy. Numerical simulations validate the theoretical findings, confirming that both the energy and amplitude detectors achieve the minimum error probability in their respective SNR domains. The proposed framework not only provides a theoretical foundation for constant-envelope signal detection but also offers a low-complexity implementation pathway, making it highly suitable for resource-constrained and interference-limited communication environments.

Index Terms—signal detection, noncoherent detection, energy detection, amplitude detection.

I. INTRODUCTION

Signal detection plays a crucial role in modern communication systems, ensuring reliable and efficient data transmission. The ability to detect signals accurately amidst noise and interference is fundamental, particularly as communication

systems continue to evolve in complexity and capability [1]–[8].

In the realm of signal detection, much attention has been given to signals with arbitrary envelopes, random distributions, and various other characteristics [9]–[11]. Here, we focus on the detection of constant-envelope signals due to their practical applications and importance in communication systems [12]–[16]. Constant-envelope signals, which maintain a consistent amplitude irrespective of the information they convey, are vital across several domains due to their advantages in hardware friendliness, energy efficiency, and communication reliability. For instance, in Internet of Things (IoT) applications, devices require low-power, simple receivers for signal detection. This requirement motivates the use of constant-envelope signals compatible with energy-efficient amplification, making them particularly suitable for activation signals [17]–[19]. Meanwhile, in wireless sensor networks (WSNs), constant-envelope signals are widely used to enable efficient device activation and localization. Their properties enhance range and sensing capabilities while conserving power and extending system duration [20], [21].

Typically, coherent detection methods generally offer superior performance in signal detection, as they can extract both amplitude and phase information from the received signal. In systems using IQ demodulators, the incoming modulated signal is split into its in-phase and quadrature components by mixing with two local oscillator signals that are 90 degrees out of phase with each other. This allows for precise amplitude and phase recovery, enabling efficient signal processing [9]–[11], [15], [22], [23]. However, this matching process introduces significant complexity and resource demands in hardware design, particularly due to the need for precise frequency and phase matching to ensure proper separation and reconstruction of the IQ components of the signal.

With the increasing demand for simpler, resource-efficient receivers, particularly for the noncoherent detection of constant-envelope signals where devices often only need to

detect the presence of signals rather than demodulate all information [12], [24], alternative detection structures are sought. The BFED presents a compelling simplified receiver design [25]. In this paper, we demonstrate that BFED can effectively detect constant-envelope signals by matching them with a known reference to maximize energy, thereby operating across a wide frequency band and eliminating the need for precise frequency matching. We also show that with the BFED, amplitudes can be estimated using only magnitudes with a simpler maximum likelihood estimator (MLE), thus significantly reducing the complexity of the receiver structure compared to traditional methods [26]. These results illustrate how BFED provides a practical and efficient solution for constant-envelope signal detection, particularly in resource-constrained environments.

While BFED offers a practical solution for constant-envelope signal detection in resource-constrained environments, it raises an important theoretical question: is the energy detector truly the optimal noncoherent detection statistic, or could better decision metrics be derived? Traditional approaches often assume that the optimal noncoherent detector reduces to a simple energy detector, based on the structure of IQ demodulators, without a rigorous formal proof [10], [15], [22], [24]. This creates a critical gap in the theory, as it remains unclear whether more effective detection strategies can be formulated from first principles. In this work, we revisit the noncoherent detection framework, beginning directly from the envelope-detected output—the sequence of noisy received signal magnitudes—while discarding any phase information. By carefully re-deriving the optimal detector from these magnitude-only observations, we not only provide the first rigorous justification for the energy detector’s optimality in the low SNR regime, but we also uncover a novel amplitude-based detector structure that emerges at high SNR. This rigorous treatment not only resolves longstanding questions in noncoherent detection theory but also lays the groundwork for more efficient and insightful receiver designs tailored to constant-envelope signalling.

Motivated by these considerations, we draw upon established statistical tests to systematically determine the optimum decision rules. Two statistical tests are generally utilized in this derivation: the Neyman-Pearson (NP) test and the Bayesian test [25]. The NP test maximizes the detection probability for a specified false alarm rate, making it the most powerful test for balancing detection and false alarm trade-offs at each point along the Receiver Operating Characteristic (ROC) curve. However, it does not directly minimize the overall error probability, which can be a limitation in certain applications where both types of errors are equally important. If we have the prior knowledge about the probabilities of the hypotheses and the costs associated with different decision outcomes, Bayesian is a better approach, which can lead directly to the optimum decision threshold, and achieves the optimum probability of error. This approach allows us to design a detector that is more robust and efficient for a wide range of practical communication scenarios.

We assume that the noise power spectral density at the receiver is known, as it can be easily measured when no signal is present. However, in communication systems, the amplitudes often need to be estimated online due to the information or physical meaning they convey. For example, in Integrated Sensing and Communication (ISAC) systems, the estimation of signal amplitudes is related to target distance and reflection environments, making it essential to accurately estimate them [1], [27]. Thus, the amplitude of constant-envelope signals needs to be estimated using MLE based on the magnitudes of the noisy received signals obtained from the previous simple receiver design, as investigated in our prior work [26]. To address this, we employ the GLRT to derive the optimal detector, which allows for effective hypothesis testing even when signal parameters are not fully known. The unknown amplitudes are estimated using MLE, and a likelihood ratio test is then formed based on these estimates.

In this paper, we develop and analyse the procedures to achieve optimal detection of constant-envelope signals by leveraging the received signal magnitudes. We focus on a hardware-lightweight solution using the BFED to detect signal amplitudes, particularly in resource-constrained environments. Building on the constant-envelope signal model, we formulate the detection problem using Bayesian principles and the GLRT. The nonlinear nature of the GLRT leads us to approximate Bessel functions and separately address detection in the low and high SNR regimes, leading to distinct detection strategies for each. For low SNR, we derive an energy detector, an approach commonly used in traditional signal detection. However, we make a significant contribution by firstly providing a rigorous theoretical proof of the energy detector’s optimality in this regime, underpinned by Bayesian test. This allows us to determine the precise detection threshold, ensuring maximum detection reliability while minimizing the error probability. In contrast, for high SNR, we derive a new detector that incorporates MLE of the signal amplitude. This detector compares the estimated amplitude to the standard deviation to perform detection, offering improved performance over traditional detectors in this regime. Through a combination of analysis and extensive numerical simulations, we validate the effectiveness of these detectors across a range of noise conditions, demonstrating their robustness and the superior performance of the new high SNR detector. Our findings contribute to the field by offering a rigorous, unified approach to constant-envelope signal detection that bridges theory and practical implementation.

The paper is organized as follows. Section II describes the signal model and the derivation of the optimal detection rule using GLRT. In Section III, we analyse the performance of the Energy Detector (ED) and the Amplitude Detector (AD). Section IV presents numerical simulations to validate the effectiveness of these detectors, and Section V gives some concluding remarks.

II. DETECTION BASED ON RECEIVED SIGNAL MAGNITUDE

A. Received Signal Model

We consider the problem of detecting a constant envelope signal with circularly symmetric complex Gaussian (CSCG) noise. The binary hypothesis testing problem of the received signal can be formulated as

$$H_1: r(k) = Ae^{j(\omega k + \theta)} + n(k), \quad k = 0, 1, \dots, N-1 \quad (1)$$

$$H_0: r(k) = n(k), \quad k = 0, 1, \dots, N-1 \quad (2)$$

where A is the amplitude of the signal, N is the number of samples, ω is the frequency of the signal, θ is the phase of the signal and $n(k)$ is complex additive white Gaussian noise (AWGN) with zero mean and variance $2\sigma^2$, which is assumed as prior knowledge here. H_1 assumes the presence of a signal, while H_0 represents the case where only noise is present. The SNR level here is defined as $\rho = \frac{A^2}{2\sigma^2}$.

For the simplified noncoherent receiver, we apply the BFED to the received signal model $r(k)$, which structure is a band-pass filter connected with an envelope detector. BFED can effectively extract the signal's envelope without the complexities introduced by frequency and phase variations. The end result of this process is $\{|r(k)|\}_{k=0}^{N-1}$, which is a simplified signal representation that emphasizes amplitude, easing subsequent processing steps. And we will derive the optimal detector start from this representation.

From (2), the distribution of the amplitude of received signal $|r(k)|$ under H_1 follows a Rician distribution with the parameter A and σ , and the joint probability density function of all the received samples $\{|r(k)|\}_{k=0}^{N-1}$ conditioned on the unknown amplitude A can be derived as

$$\begin{aligned} & P\left(\{|r(k)|\}_{k=0}^{N-1} \mid H_1, A\right) \\ &= \prod_{k=0}^{N-1} \frac{|r(k)|}{\sigma^2} \exp\left(-\frac{|r(k)|^2 + A^2}{2\sigma^2}\right) I_0\left(\frac{|r(k)|A}{\sigma^2}\right) \end{aligned} \quad (3)$$

where the $I_v(\cdot)$ is the first kind modified Bessel function. Meanwhile, $|r(k)|$ under H_0 follows a Rayleigh distribution, and the joint PDF of samples is

$$P\left(\{|r(k)|\}_{k=0}^{N-1} \mid H_0\right) = \prod_{k=0}^{N-1} \frac{|r(k)|}{\sigma^2} \exp\left(-\frac{|r(k)|^2}{2\sigma^2}\right) \quad (4)$$

while the corresponding log-likelihood functions are

$$\begin{aligned} H_1: \quad & \ln \mathcal{L}(H_1; A) \\ &= -N \ln(\sigma^2) + \sum_{k=0}^{N-1} \ln |r(k)| - \frac{NA^2}{2\sigma^2} \\ &\quad - \frac{1}{2\sigma^2} \sum_{k=0}^{N-1} |r(k)|^2 + \sum_{k=0}^{N-1} \ln I_0\left(\frac{|r(k)|A}{\sigma^2}\right) \end{aligned} \quad (5)$$

$$\begin{aligned} H_0: \quad & \ln \mathcal{L}(H_0) \\ &= -N \ln(\sigma^2) + \sum_{k=0}^{N-1} \ln |r(k)| - \frac{1}{2\sigma^2} \sum_{k=0}^{N-1} |r(k)|^2. \end{aligned} \quad (6)$$

B. Generalized Likelihood Ratio Test

According to the Bayesian test, we want to derive the optimum detector with the minimum probability of error

$$P_e = P(H_0|H_1)P(H_1) + P(H_1|H_0)P(H_0). \quad (7)$$

To minimize the P_e , we apply the likelihood ratio test by comparing the likelihood ratio to a threshold. Here, if the likelihood for H_1 is higher, we decide in favor of H_1 , and vice versa.

Besides, because the amplitude of the received signal is unknown, the optimal detection performance can be achieved by the GLRT. The unknown amplitude A are determined by the MLE. Based on the likelihood calculated from (3) and (4), the GLRT is given by

$$\Lambda = \frac{\max_A P\left(\{|r(k)|\}_{k=0}^{N-1} \mid H_1, A\right)}{P\left(\{|r(k)|\}_{k=0}^{N-1} \mid H_0\right)} \underset{H_0}{\overset{H_1}{\gtrless}} 1 \quad (8)$$

which can be formulated as

$$\Lambda = \frac{P\left(\{|r(k)|\}_{k=0}^{N-1} \mid H_1, \hat{A}\right)}{P\left(\{|r(k)|\}_{k=0}^{N-1} \mid H_0\right)} \underset{H_0}{\overset{H_1}{\gtrless}} 1 \quad (9)$$

where \hat{A} is the MLE of the amplitude. Take the logarithms and the simplifying yields

$$\ln \Lambda = -\frac{N\hat{A}^2}{2\sigma^2} + \sum_{k=0}^{N-1} \ln I_0\left(\frac{|r(k)|\hat{A}}{\sigma^2}\right) \underset{H_0}{\overset{H_1}{\gtrless}} 0. \quad (10)$$

To find \hat{A} , we need to maximize $\ln \mathcal{L}(H_1; A)$ with respect to A . The derivate of $\ln \Lambda$ with respect to A is

$$\frac{d}{d\hat{A}} \ln \Lambda = -\frac{N\hat{A}}{\sigma^2} + \sum_{k=0}^{N-1} \frac{I_1\left(\frac{|r(k)|\hat{A}}{\sigma^2}\right)}{I_0\left(\frac{|r(k)|\hat{A}}{\sigma^2}\right)} \cdot \frac{|r(k)|}{\sigma^2} = 0 \quad (11)$$

which yields

$$\hat{A} = \frac{1}{N} \sum_{k=0}^{N-1} \frac{|r(k)| I_1\left(\frac{|r(k)|\hat{A}}{\sigma^2}\right)}{I_0\left(\frac{|r(k)|\hat{A}}{\sigma^2}\right)}. \quad (12)$$

Due to the nonlinear property of the first kind modified Bessel function, we cannot directly derive a closed-form of \hat{A} . We will discuss the approximation of the $I_v(\cdot)$ in the low SNR case and high SNR case separately to derive an analytic expression in the following parts.

C. Low SNR Case

For $I_0(x)$, when the variable x is close to 0, its approximation can be expressed as

$$I_0(x) \approx 1 + \frac{x^2}{4} \quad (13)$$

and for the very small x we also have $\ln(1+x) \approx x$, thus we have

$$\ln I_0(x) \approx \frac{x^2}{4} \quad (14)$$

and with those approximations, we can simplify the GLRT in (10) as

$$\begin{aligned}
\ln \Lambda &= -\frac{N\hat{A}^2}{2\sigma^2} + \sum_{k=0}^{N-1} \ln I_0 \left(\frac{|r(k)|\hat{A}}{\sigma^2} \right) \\
&= -\frac{N\hat{A}^2}{2\sigma^2} + \sum_{k=0}^{N-1} \frac{\left(\frac{|r(k)|\hat{A}}{\sigma^2} \right)^2}{4} \\
&= -\frac{N\hat{A}^2}{2\sigma^2} + \frac{\hat{A}^2}{4\sigma^4} \sum_{k=0}^{N-1} |r(k)|^2 \\
&\stackrel{H_1}{\geq} \underset{H_0}{0}
\end{aligned} \tag{15}$$

which is finally equivalent to

$$E = \frac{1}{N} \sum_{k=0}^{N-1} |r(k)|^2 \stackrel{H_1}{\geq} \underset{H_0}{2\sigma^2}. \tag{16}$$

In the low SNR regime, the above analysis reveals that the optimal detection strategy simplifies into an energy detection scheme. Specifically, by approximating the modified Bessel function, the complex likelihood ratio test reduces to comparing the average received energy E against the noise energy level $2\sigma^2$. This outcome is significant: while energy detectors are often employed as the test statistic, here we first derive it rigorously as the optimal solution for minimizing the overall error probability at low SNR. Thus, rather than being a merely heuristic, the energy detector emerges naturally from the fundamental statistical properties of the problem, confirming its optimality in scenarios where the signal is weak relative to the noise.

D. High SNR Case

For $I_\nu(x)$, when the variable x is very large, it can be expressed as

$$I_0(x) \approx \frac{e^x}{\sqrt{2\pi x}} \left[1 + \frac{1}{8x} \left(1 + \frac{9}{2(8x)} (1 + \dots) \right) \right] \tag{17}$$

$$I_1(x) \approx \frac{e^x}{\sqrt{2\pi x}} \left[1 - \frac{3}{8x} \left(1 + \frac{5}{2(8x)} (1 + \dots) \right) \right] \tag{18}$$

and thus the Bessel function ratio in (12) can be approximated

$$\frac{I_1(x)}{I_0(x)} \approx 1 - \frac{4}{8x + 1} \approx 1 - \frac{1}{2x} \tag{19}$$

With those approximations, the solution of the MLE for (12) can be simplified as the solution of the following equation [26]:

$$\hat{A}^2 - \frac{1}{N} \sum_{k=0}^{N-1} |r(k)|\hat{A} + \frac{\sigma^2}{2} = 0. \tag{20}$$

For simplification, let

$$R = \frac{1}{N} \sum_{k=1}^N |r(k)| \tag{21}$$

and the MLE of amplitude can be solved as

$$\hat{A}_{LA} = \frac{1}{2}R \pm \frac{1}{2}\sqrt{R^2 - 2\sigma^2}. \tag{22}$$

For large argument approximation where $R^2 \gg 2\sigma^2$, the solution with the $-$ sign results in an estimate approaching zero. The solution with the $+$ sign is close to R and is more realistic. Simulations show that, in the case of large noise, rare occasions with $R^2 - 2\sigma^2 < 0$ occur, resulting in complex solutions to the quadratic equation in (22). Hence, we propose to take the real part of (22) as the amplitude estimator

$$\hat{A}_{LAR} = \frac{1}{2} \left(R + \text{Re} \left[\sqrt{R^2 - 2\sigma^2} \right] \right). \tag{23}$$

Now we can use the MLE result \hat{A}_{LAR} to simplify the GLRT from (10). When the parameter x is very large, the logarithm of $I_0(x)$ has an approximation

$$\begin{aligned}
\ln I_0(x) &\approx \ln \left\{ \frac{e^x}{\sqrt{2\pi x}} \left[1 + \frac{1}{8x} \left(1 + \frac{9}{2(8x)} (1 + \dots) \right) \right] \right\} \\
&\approx x - \frac{1}{2} \ln(2\pi x) \\
&\approx x
\end{aligned} \tag{24}$$

and thus the test statistic (10) can be simplified as

$$\begin{aligned}
\ln \Lambda &= -\frac{N\hat{A}_{LAR}^2}{2\sigma^2} + \sum_{k=0}^{N-1} \ln I_0 \left(\frac{|r(k)|\hat{A}_{LAR}}{\sigma^2} \right) \\
&\approx -\frac{N\hat{A}_{LAR}^2}{2\sigma^2} + \sum_{k=0}^{N-1} \frac{|r(k)|\hat{A}_{LAR}}{\sigma^2} \\
&= -\frac{N\hat{A}_{LAR}^2}{2\sigma^2} + \frac{\hat{A}_{LAR}}{\sigma^2} \sum_{k=0}^{N-1} |r(k)| \\
&\stackrel{H_1}{\geq} \underset{H_0}{0}.
\end{aligned} \tag{25}$$

Using the result in (20), it can be is simplified as

$$\begin{aligned}
\ln \Lambda &= \frac{N}{2\sigma^2} \left(2\hat{A}_{LAR} \sum_{k=0}^{N-1} |r(k)| - \hat{A}_{LAR}^2 \right) \\
&= \frac{N}{2\sigma^2} \left(\hat{A}_{LAR}^2 - \sigma^2 \right) \\
&\stackrel{H_1}{\geq} \underset{H_0}{0}
\end{aligned} \tag{26}$$

where the result can be derived as

$$\hat{A}_{LAR} \stackrel{H_1}{\geq} \underset{H_0}{\sigma}. \tag{27}$$

Here, we can further simplify (27) by analyzing the square root item of \hat{A}_{LAR} . Recall \hat{A}_{LAR} in (23), when the inner square root part of \hat{A}_{LAR} is real ($R^2 \geq 2\sigma^2$), we can show that the amplitude detector can be simplified as

$$R \stackrel{H_1}{\geq} \underset{H_0}{\frac{3}{2}\sigma} \tag{28}$$

When $R^2 < 2\sigma^2$, the square root is imaginary, and we take the real part:

$$\hat{A}_{\text{LAr}} = \frac{1}{2}R \quad (29)$$

Since $R < \sqrt{2}\sigma$, $\hat{A}_{\text{LAr}} < \sigma$, so the decision is H_0 . Thus, the amplitude detector can be translated into a threshold on R :

$$R \underset{H_0}{\overset{H_1}{\geq}} \frac{3}{2}\sigma. \quad (30)$$

As shown in (30), in the high SNR scenario, the derived optimal detector takes the form of an amplitude detector, which compares the sample mean of the signal amplitude directly against the noise standard deviation $\frac{3}{2}\sigma$.

Here, we first derive the optimum detection framework by working exclusively with the noisy received signal magnitudes $\{|r(k)|\}_{k=0}^{N-1}$ and employing a magnitude estimation. Our new detector circumvents the need for precise frequency alignment and complex baseband processing. Both the optimum detectors derived in low and high SNR stands in stark contrast to traditional IQ-based detection methods, which require phase synchronization and detailed frequency estimates. Our derivation proves that at low SNR, energy detector provides the optimal solution, while at high SNR, an amplitude detector is theoretical optimum.

III. PERFORMANCE ANALYSIS

A. Performance Analysis of the Energy Detector

In this section, we presents the derivation of the false alarm rate P_{FA} and misdetection rate P_{MD} for the proposed energy detector to further calculate the probability of error P_e . The amplitude detector decides between the presence or absence of a signal based on the energy E . The detailed derivation includes distribution analysis under both hypotheses H_0 and H_1 , and expresses P_{FA} and P_{MD} properly.

1) *Probability of False Alarm:* For the energy detector in low SNR case, the null hypothesis H_0 is

$$H_0 : r(k) = n(k), \quad k = 0, 1, \dots, N-1$$

and the test statistic denoted as E is

$$\begin{aligned} E &= \frac{1}{N} \sum_{k=0}^{N-1} |r(k)|^2 \\ &= \frac{1}{N} \sum_{k=0}^{N-1} |n(k)|^2 \\ &= \frac{1}{N} \sum_{k=0}^{N-1} (n_I^2(k) + n_Q^2(k)). \end{aligned} \quad (31)$$

Since $n_I(k)$ and $n_Q(k)$ are independent Gaussian random variables with zero mean and variance σ^2 , the sum $n_I^2(k) + n_Q^2(k)$ follows an exponential distribution with mean $2\sigma^2$. Therefore, E is the average of N independent exponential random variables, which follows a gamma distribution

$$E \sim \text{Gamma}\left(N, \frac{2\sigma^2}{N}\right) \quad (32)$$

with shape parameter $\alpha = N$ and scale parameter $\theta = \frac{2\sigma^2}{N}$. And we can calculate the mean and variance of E under H_0 as

$$\mu_E = \mathbb{E}[E | H_0] = N\theta = 2\sigma^2 \quad (33)$$

$$\sigma_E^2 = \text{Var}[E | H_0] = N\theta^2 = \frac{4\sigma^4}{N}. \quad (34)$$

The probability of false alarm is the probability that E exceeds the detection threshold $2\sigma^2$ under H_0 , which is

$$P_{\text{FA}} = 1 - F_E(2\sigma^2 | H_0) \quad (35)$$

where F_E is the cumulative distribution function (CDF) of E under H_0 . And then we use the CDF of the gamma distribution

$$F_E(2\sigma^2 | H_0) = \frac{\gamma(N, N)}{\Gamma(N)} \quad (36)$$

where $\Gamma(N)$ is the Gamma function and $\gamma(N, z)$ is the lower incomplete gamma function:

$$\Gamma(N) = (N-1)! \quad (37)$$

$$\gamma(N, N) = \int_0^N t^{N-1} e^{-t} dt. \quad (38)$$

According to this, we can derive that the false alarm rate for ED is

$$P_{\text{FA}} = 1 - \frac{\gamma(N, N)}{\Gamma(N)}. \quad (39)$$

2) *Probability of Misdetection:* The signal under H_1 is

$$H_1 : r(k) = Ae^{j(\omega k + \theta)} + n(k), \quad k = 0, 1, \dots, N-1$$

We first analyse the distribution of $|r(k)|^2$. The complex signal $Ae^{j(\omega k + \theta)}$ and noise $n(k)$ can be decomposed into their real and imaginary components

$$s(k) = A \cos(\omega k + \theta) + jA \sin(\omega k + \theta) \quad (40)$$

$$n(k) = n_I(k) + jn_Q(k) \quad (41)$$

where $n_I(k)$ and $n_Q(k)$ are independent zero-mean Gaussian random variables with variance σ^2 .

Thus, the received signal can be written as

$$r(k) = [A \cos(\omega k + \theta) + n_I(k)] + j[A \sin(\omega k + \theta) + n_Q(k)] \quad (42)$$

with means

$$\mu_I = A \cos(\omega k + \theta) \quad (43)$$

$$\mu_Q = A \sin(\omega k + \theta) \quad (44)$$

and variances σ^2 . We can derive that

$$|r(k)|^2 = [r_I(k)]^2 + [r_Q(k)]^2. \quad (45)$$

This expression represents the sum of the squares of two independent Gaussian random variables Z_I and Z_Q with non-zero means and equal variances:

$$\mu_{Z_I} = \frac{\mu_I}{\sigma} = \frac{A \cos(\omega k + \theta)}{\sigma} \quad (46)$$

$$\mu_{Z_Q} = \frac{\mu_Q}{\sigma} = \frac{A \sin(\omega k + \theta)}{\sigma}. \quad (47)$$

Thus, the $|r(k)|^2$ follows a non-central chi-squared distribution with 2 degrees of freedom and the non-centrality parameter:

$$\lambda = \mu_{Z_1}^2 + \mu_{Z_Q}^2 = \frac{A^2}{\sigma^2} \quad (48)$$

and we can conclude that

$$\left(\frac{r_I(k)}{\sigma}\right)^2 + \left(\frac{r_Q(k)}{\sigma}\right)^2 \sim \chi_2'^2(\lambda) \quad (49)$$

and thus

$$[r_I(k)]^2 + [r_Q(k)]^2 = |r(k)|^2 \sim \sigma^2 \chi_2'^2(\lambda). \quad (50)$$

Then, we can derive the distribution of test statistic E under H_1 as

$$\begin{aligned} E &= \frac{1}{N} \sum_{k=0}^{N-1} \left| A e^{j(\omega k + \theta)} + n(k) \right|^2 \\ &= \frac{1}{N} \sum_{k=0}^{N-1} \left(A^2 + 2A \operatorname{Re} \left\{ e^{-j(\omega k + \theta)} n(k) \right\} + |n(k)|^2 \right). \end{aligned} \quad (51)$$

Since $n(k)$ is complex Gaussian noise with zero mean, the cross-term $\operatorname{Re} \left\{ e^{-j(\omega k + \theta)} n(k) \right\}$ has zero mean and variance σ^2 . Therefore, the expected value of E under H_1 can be derived as

$$\mu_E = \mathbb{E}[E | H_1] = A^2 + 2\sigma^2. \quad (52)$$

To find the distribution of E under H_1 , we have $|r(k)|^2 \sim \sigma^2 \chi_2'^2(\lambda)$ from (50). Therefore, the sum $\sum_{k=0}^{N-1} |r(k)|^2$ follows a non-central chi-squared distribution with $2N$ degrees of freedom and non-centrality parameter $\Lambda = N\lambda = \frac{NA^2}{\sigma^2}$:

$$\sum_{k=0}^{N-1} |r(k)|^2 \sim \sigma^2 \cdot \chi_{2N}'^2\left(\frac{NA^2}{\sigma^2}\right). \quad (53)$$

Therefore, the test statistic E under H_1 is:

$$E | H_1 \sim \frac{\sigma^2}{N} \cdot \chi_{2N}'^2\left(\frac{NA^2}{\sigma^2}\right). \quad (54)$$

The mean and variance of E under H_1 are:

$$\mu_E = \mathbb{E}[E | H_1] = \frac{\sigma^2}{N} \left(2N + \frac{NA^2}{\sigma^2} \right) = \sigma^2 + A^2 \quad (55)$$

$$\sigma_E^2 = \operatorname{Var}[E | H_1] = 2 \frac{\sigma^4}{N^2} \left(2N + 2 \frac{NA^2}{\sigma^2} \right) = \frac{4\sigma^4 + 4\sigma^2 A^2}{N}. \quad (56)$$

The probability of misdetection is the probability that E falls below the threshold $2\sigma^2$ under H_1 :

$$P_{MD} = F_E(2\sigma^2 | H_1). \quad (57)$$

Using the cumulative distribution function of the non-central chi-squared distribution:

$$P_{MD} = 1 - Q_N\left(\frac{A}{\sigma}\sqrt{N}, \sqrt{2N}\right) \quad (58)$$

where $Q_N(a, b)$ is the generalized Marcum Q-function

$$Q_N(a, b) = \int_b^\infty x \left(\frac{x}{a}\right)^{N-1} \exp\left(-\frac{x^2 + a^2}{2}\right) I_{N-1}(ax) dx. \quad (59)$$

Thus, according to (39) and (58), the probability of error for energy detector is

$$\begin{aligned} P_e &= P_{MD}P(H_1) + P_{FA}P(H_0) \\ &= \frac{1}{2} \left(2 - \frac{\gamma(N, N)}{\Gamma(N)} - Q_N\left(\frac{A}{\sigma}\sqrt{N}, \sqrt{2N}\right) \right) \end{aligned} \quad (60)$$

B. Performance Analysis of the Amplitude Detector

In this section, we present the derivation of the false alarm rate P_{FA} and misdetection rate P_{MD} for the proposed amplitude detector to further calculate the probability of error P_e . The amplitude detector decides between the presence or absence of a signal based on the estimated amplitude R calculated from received signal magnitudes. The detailed derivation includes approximations under both hypotheses H_0 and H_1 , and expresses P_{FA} and P_{MD} using appropriate statistical distributions.

1) *Probability of False Alarm:* Under hypothesis H_0 , $r(k) = n(k)$, the magnitude $|r(k)|$ follows a Rayleigh distribution with the probability density function (PDF):

$$f_{|r|}(x) = \frac{x}{\sigma^2} e^{-\frac{x^2}{2\sigma^2}}, \quad x \geq 0. \quad (61)$$

We consider the sum of the magnitudes over N samples:

$$S = \sum_{k=1}^N |r(k)|. \quad (62)$$

Our goal is to find the CDF of the test statistic S or R and thus calculate the outage probability. The sum S of Rayleigh-distributed random variables does not have a simple closed-form PDF. However, in [28], a modified CDF approximation for the sum of Rayleigh random variables is given.

$$F_S(x) = F_{SAA}(x) - F_{\text{error}}(x) \quad (63)$$

where $F_{SAA}(t)$ is the small argument approximation (SAA) for the sum CDF

$$F_{SAA}(x) = 1 - e^{-\frac{x^2}{2bN\sigma^2}} \sum_{k=0}^{N-1} \frac{\left(\frac{x^2}{2bN\sigma^2}\right)^k}{k!} \quad (64)$$

$$b = \frac{\sigma^2}{N} ((2N-1)!)^{1/N} \quad (65)$$

where $(2N-1)!! = (2N-1) \times (2N-3) \times \dots \times 3 \times 1$.

The difference item $F_{\text{error}}(x)$ is an empirically difference from the SAA approximation to the real value, which is

$$F_{\text{error}}(x) \approx \frac{a_0 \cdot x \left(x - a_2 \sigma \sqrt{N}\right)^{2N-1} \exp\left(-\frac{a_1(x - a_2 \sigma \sqrt{N})^2}{2\sigma^2 N b}\right)}{\left(\sigma \sqrt{N}\right)^{2N} \cdot 2^{N-1} \left(\frac{b}{a_1}\right)^N N!} \quad (66)$$

where the coefficients a_0, a_1, a_2 are calculated by fitting the error function to the difference between the Rayleigh sum variables' CDF and the F_{SAA} .

Thus, the P_{FA} is defined as the probability that the sum S exceeds the threshold under H_0 is given by

$$\begin{aligned} P_{\text{FA}} &= 1 - F_S \left(\frac{3}{2} N \sigma \right) \\ &= 1 - \left[F_{\text{SAA}} \left(\frac{3}{2} N \sigma \right) - F_{\text{error}} \left(\frac{3}{2} N \sigma \right) \right]. \end{aligned} \quad (67)$$

2) *Probability of Misdetction:* Under hypothesis H_1 , $r(k) = A e^{j(\omega k + \theta)} + n(k)$. The magnitude $|r(k)|$ follows a Ricean distribution with PDF

$$f_{|r|}(x) = \frac{x}{\sigma^2} e^{-\frac{x^2 + A^2}{2\sigma^2}} I_0 \left(\frac{x A}{\sigma^2} \right), \quad x \geq 0, \quad (68)$$

The misdetection rate is denoted by

$$P_{\text{MD}} = P \left(S < \frac{3}{2} N \sigma \mid H_1 \right). \quad (69)$$

However, the Ricean sum random variables also don't have a closed-form representation. From [29], the cdf for the sum of N i.i.d. Ricean random variables S is given by:

$$F_S(r) = \frac{1}{\sigma^{2N}} \exp \left(-\frac{\nu^2 N}{2\sigma^2} \right) \sum_{i=0}^{\infty} \frac{\delta_i r^{2(i+N)}}{\Gamma(2(i+N)+1)} \quad (70)$$

where $\nu = \frac{A}{\sigma}$ is the Rice factor and δ_i are recursively calculated coefficients computed recursively by

$$\begin{aligned} \delta_0 &= 1 \\ \delta_i &= \frac{1}{i} \sum_{k=1}^i (Nk + k - i) \delta_{i-k} \sum_{l=0}^k \frac{\Gamma(2(k+1))}{(2\sigma^2)^l \left(\frac{\nu}{2\sigma^2} \right)^{2(k-l)} (k-l)! l!} \end{aligned} \quad (71)$$

where $\Gamma(\cdot)$ is the gamma function, N is the number of samples at the receiver, and σ and ν are the parameters as defined above.

To find P_{MD} , we substitute the threshold $r = \frac{3}{2} N \sigma$ in $F_S(r)$:

$$\begin{aligned} P_{\text{MD}} &= F_S \left(\frac{3}{2} N \sigma \right) \\ &= \frac{1}{\sigma^{2N}} \exp \left(-\frac{\nu^2 N}{2\sigma^2} \right) \sum_{i=0}^{\infty} \frac{\delta_i \left(\frac{3}{2} N \sigma \right)^{2(i+N)}}{\Gamma(2(i+N)+1)}. \end{aligned} \quad (73)$$

Thus, according to (67) and (73), the probability of error for energy detector is

$$\begin{aligned} P_e &= P_{\text{MD}} P(H_1) + P_{\text{FA}} P(H_0) \\ &= \frac{1}{2} \left(1 - \left[F_{\text{SAA}} \left(\frac{3}{2} N \sigma \right) - F_{\text{error}} \left(\frac{3}{2} N \sigma \right) \right] \right) \\ &\quad + \frac{1}{\sigma^{2N}} \exp \left(-\frac{\nu^2 N}{2\sigma^2} \right) \sum_{i=0}^{\infty} \frac{\delta_i \left(\frac{3}{2} N \sigma \right)^{2(i+N)}}{\Gamma(2(i+N)+1)}. \end{aligned} \quad (74)$$

IV. NUMERICAL RESULTS AND DISCUSSIONS

In this section, the performance of the two proposed optimum magnitude based detectors are examined via simulations. According to the theoretical analysis of the proposed detectors, the performance of the low SNR case energy detector and the high SNR case amplitude detector is evaluated using three key metrics: P_{FA} , P_{MD} , and P_e . These metrics are analysed as functions of the number of samples N and the SNR.

Theoretical performance is compared against simulation results for both detectors. We set the noise energy $\sigma^2 = 1$, and using MATLAB to perform 10^8 rounds simulation. The theoretical P_{FA} and P_{MD} of ED have closed form expression given in (39) and (59), while the theoretical P_{FA} for the AD uses an approximated closed form for the sum of Rayleigh random variables. The P_{MD} for AD is calculated using a semi-analytical approach based on empirical CDFs of Ricean sum random variables (The approximation function in (73) provides a valid closed-form representation of the decision statistic. However, in the high SNR case, if we want to accurately approximate the Rician sum distributions, the iteratively computed constant will exceed MATLAB's maximum storable data length. Thus, we use this semi-analytical curve to represent the theoretical performance of the amplitude detector).

A. Probability of False Alarm

The probability of false alarm is presented in Fig. 1 and 2. Both the energy detector and the amplitude detector across different SNR values and varying numbers of samples N are illustrated, and the results are shown on a logarithmic scale for clarity.

Fig. 1 compares the simulated and theoretical false alarm probabilities for the ED and the AD as functions of the SNR under different sample sizes $N = 4$ and 16 . For the energy detector, both the simulated and theoretical P_{FA} curves align closely, confirming the accuracy of the analytical model. Notably, the ED's false alarm rate remains constant across the entire examined SNR range, irrespective of the number of observations N . This behavior arises because the ED's threshold, which is based on the known noise variance and does not depend on the presence or strength of the signal. As a result, changes in SNR have a negligible effect on the false alarm probability for the ED.

In contrast, the amplitude detector achieves a consistently lower P_{FA} than the ED. Both the simulated and approximated results for the AD closely coincide, indicating that the approximation technique used to model the AD's false alarm probability is highly accurate. Similar to the ED, the AD's P_{FA} remains stable with changing SNR. This stability also highlights that, once the AD's decision threshold is set with knowledge of the noise level, the likelihood of false alarms does not significantly vary with SNR.

Across all four sample sizes tested, the AD outperforms the ED in terms of P_{FA} , providing a lower false alarm rate at all SNR levels. Both the detectors' P_{FA} remains stable with changing SNR due to the threshold is a derived optimum value

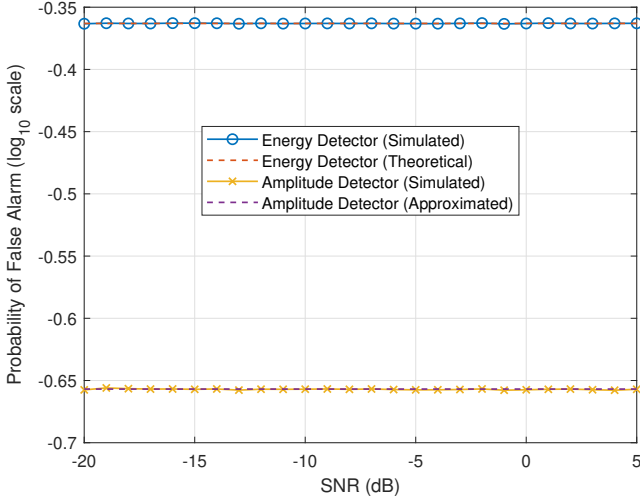
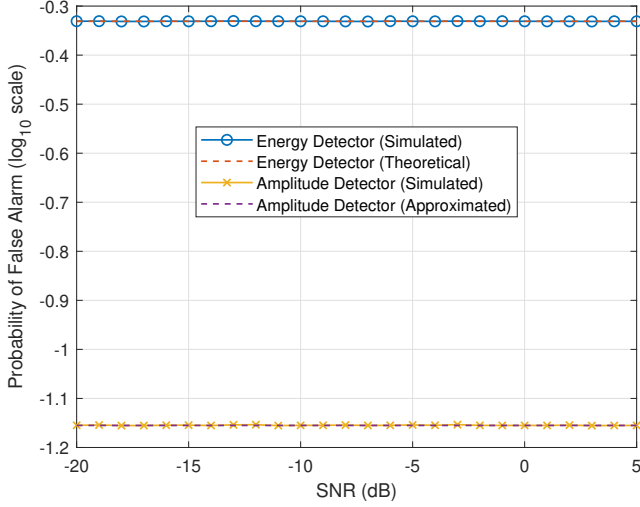
(a) $N = 4$ (b) $N = 16$

Figure 1: The probability of false alarm vs. SNR for the proposed detectors of both simulated and theoretical results.

relevant to the noise standard deviation, while the test statistics are functions of the noise and observations.

P_{FA} as a function of N for both detectors at all SNR is illustrated in Fig. 2. In this figure, the ED's simulated and theoretical curves remain close, reaffirming the analytical model's accuracy. However, the ED's false alarm probability turns bad as N grows. And finally, if the N is going to infinity, the P_{FA} of the ED will converge to a fixed value 0.5. This is due to that, with N increase to infinity, the test statistic can be approximated by a normal distribution according to Central Limit Theorem. The mean and the variance of the ED are:

$$\mu_0 = 2\sigma^2 \quad (75)$$

$$\sigma_0^2 = \frac{4\sigma^4}{N} \quad (76)$$

separately. The threshold is also the noise energy $2\sigma^2$. Thus the false alarm rate when N is very large can be calculated

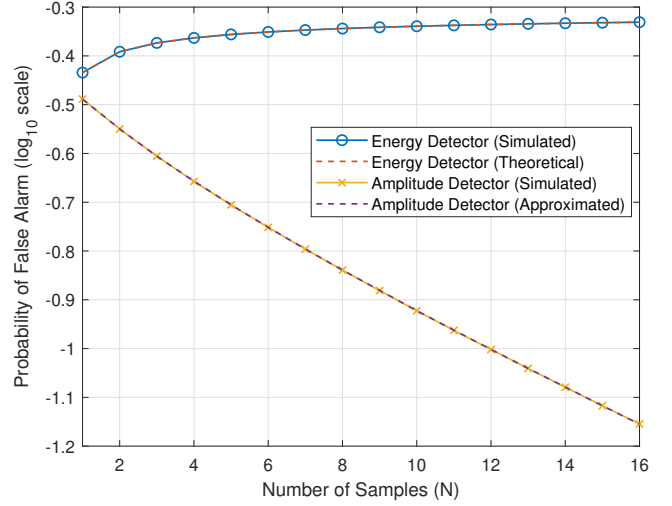


Figure 2: The probability of false alarm vs. N for the proposed detectors of both simulated and theoretical results.

by

$$P_{FA} = Q\left(\frac{2\sigma^2 - \mu_0}{\sigma_0}\right) = 0.5 \quad (77)$$

where $Q(\cdot)$ is the Q-function. This can be verified in Fig. 2, the ED is converged to $\log(0.5)$.

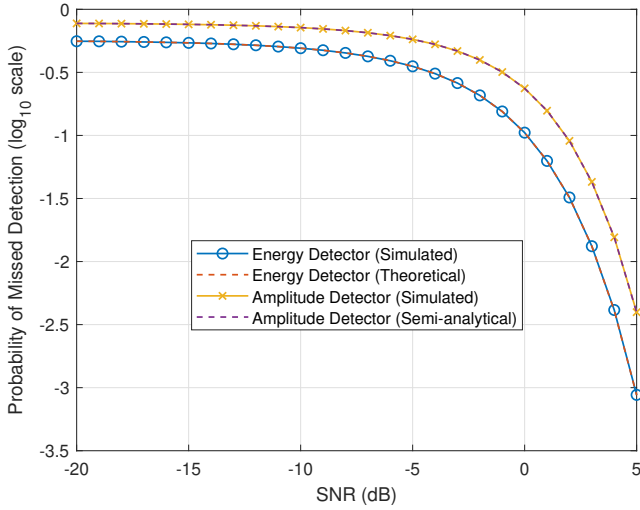
The amplitude detector exhibits a distinct advantage in terms of scalability with N . As the number of samples increases, the AD's P_{FA} decreases notably, and the simulated results closely follow the semi-analytical curve. This decrease in P_{FA} arises from the AD's reliance on amplitude estimation: more samples yield a more accurate estimate of the underlying noise distribution, refining the detector's ability to discriminate between true signal presence and noise-induced variations. Consequently, the AD leverages larger sample sizes to further suppress false alarms.

With the growth in N , the gap between the ED and AD in terms of P_{FA} widens. While the ED essentially converges at a certain false alarm level, the AD continues to improve. This divergence underscores the inherent advantage of using amplitude detection in scenarios where more samples are available, especially when stringent false alarm constraints are critical.

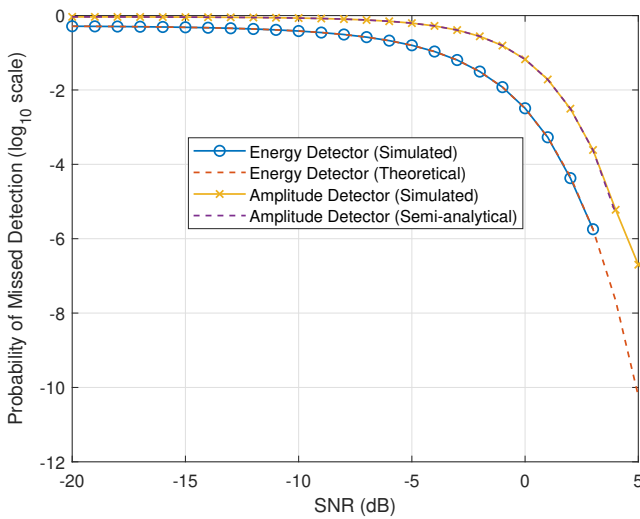
In summary, from Fig. 1 and 2, we can see that both the detectors' false alarm rate remains stable, independent of SNR and only marginally affected by the number of samples. The P_{FA} of ED is always higher than AD, and the gap increases with the N turns larger.

B. Probability of Missdetection

The misdetection probability as a function of SNR for $N = 4$ and $N = 16$ are displayed in Fig. 3. We can find that, for the both ED and AD, the simulated P_{MD} aligns closely with the derived theoretical curves across all examined SNR ranges. As the number of samples grows, both detectors exhibit improved detection capabilities. Larger N provides



(a) $N = 4$

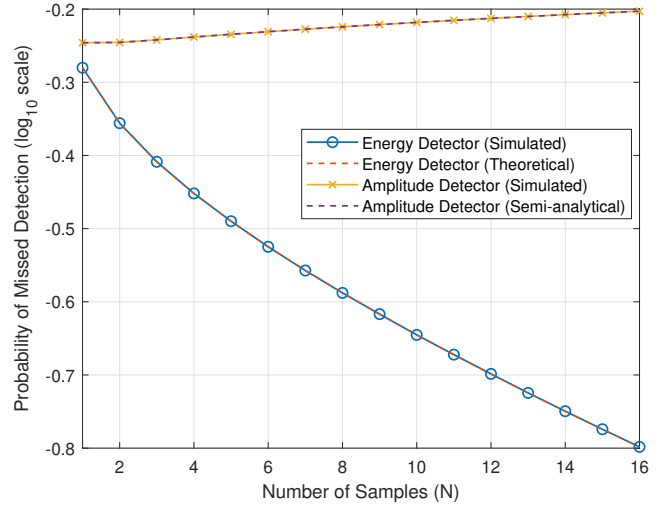


(b) $N = 16$

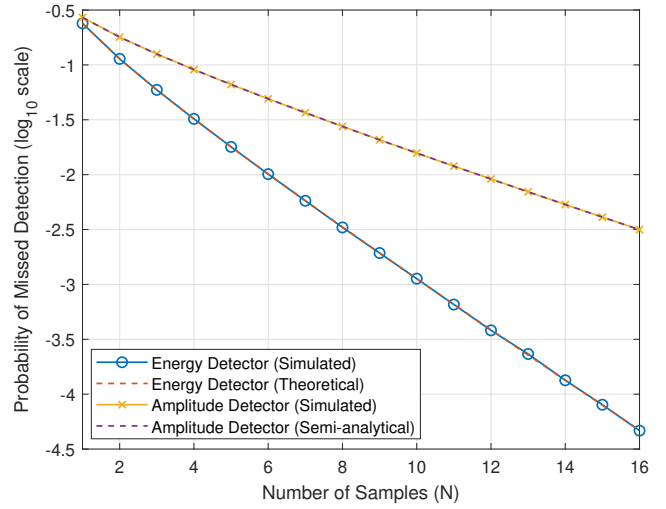
Figure 3: The probability of misdetection vs. SNR for the proposed detectors of both simulated and theoretical results.

more statistical evidence for distinguishing signal from noise, thus further decreasing P_{MD} for both ED and AD. While the ED maintains an advantage in lower SNR regimes for all N , the performance gap narrows with increasing N , especially at high SNR levels.

Fig. 4 explores the misdetection probability as the number of samples varies at fixed SNR values -5 and 2 dB. Under highly challenging conditions, the ED significantly outperforms the AD. As N increases, P_{MD} for both detectors decreases, but the ED maintains a consistently lower misdetection probability. As the SNR moves into non-negative values, the improvements in P_{MD} with increasing N become more pronounced for both detectors. Although the ED continues to yield lower misdetection probabilities, the gap between ED and AD decreases as SNR increases. This diminishing gap aligns with the theoretical prediction that the AD's amplitude estimation



(a) SNR = -5 dB



(b) SNR = 2 dB

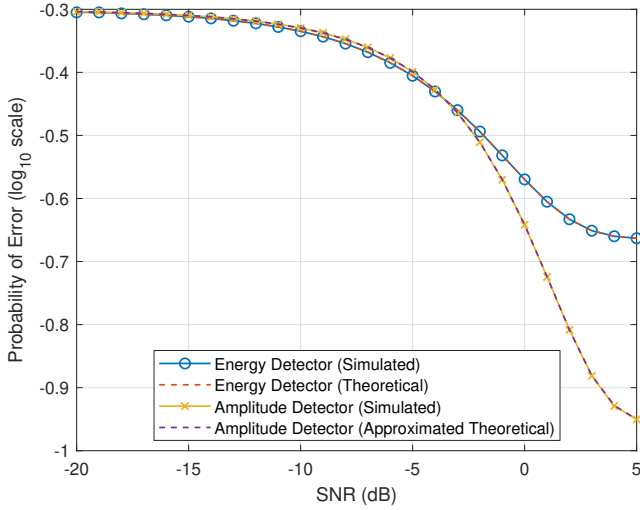
Figure 4: The probability of misdetection vs. N for the proposed detectors of both simulated and theoretical results.

mechanism becomes more reliable when the signal component is less overshadowed by noise.

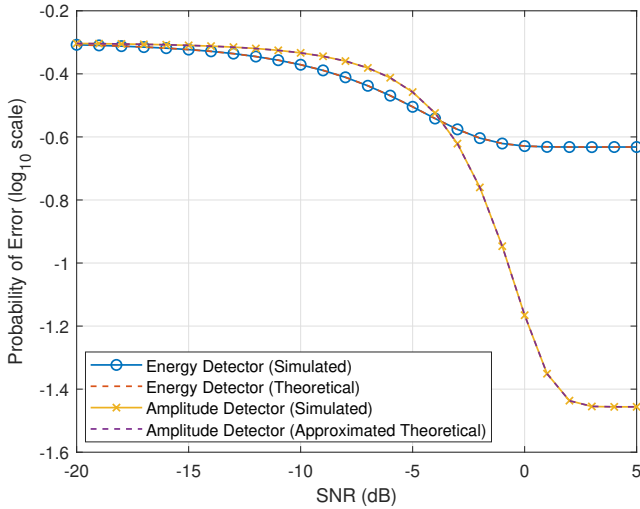
Those simulated results are consistent with the theoretical insight that the AD is not specifically optimized for low SNR scenarios. As SNR improves, the gap between ED and AD narrows. In high SNR regimes, the AD's P_{MD} draws closer to that of the ED, demonstrating that the amplitude-based strategy becomes increasingly effective when the signal amplitude estimation benefits from a stronger signal component.

C. Probability of Error

Fig. 5 shows the probability of error for $N = 4$ and 16 as the SNR varies from a low noise region to a scenario where the signal is substantially stronger than the noise. We can see that both the ED and AD's simulated results are almost same as the theoretical predictions, confirming the accuracy of the theoretical models. Besides, for all tested sample sizes, increasing SNR reduces the probability of error



(a) $N = 4$

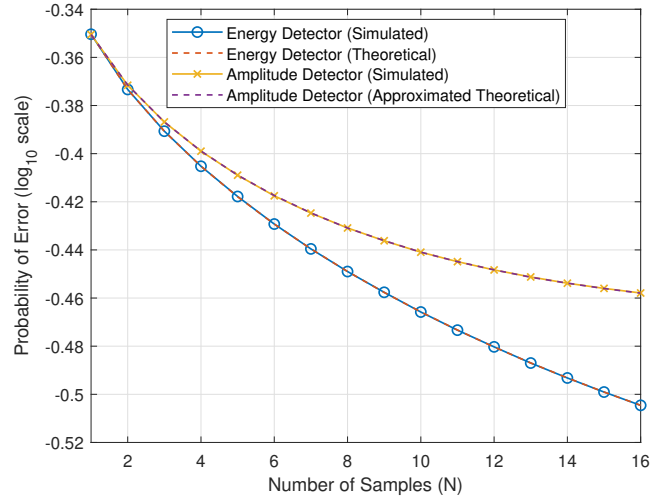


(b) $N = 16$

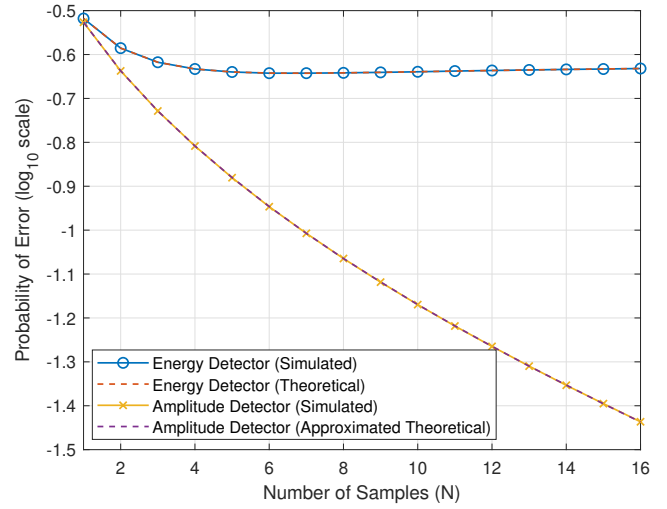
Figure 5: The probability of error vs. SNR for the proposed detectors of both simulated and theoretical results.

for both detectors, and they final converge to the value near $0.5P_{FA}$ due to that P_{MD} is much smaller with the increment of SNR.

At low SNR region, the ED maintains a lower probability of error than the AD. This aligns with the theoretical insight that the ED is derived as the optimum detector in low SNR conditions, leveraging energy accumulation to reliably detect even weak signals. In contrast, the AD initially exhibits a higher probability of error at low SNR values. As SNR improves, the AD's error curve declines more rapidly. Beyond a certain SNR threshold (around -4 to -3 dB) this rapid drop allows the AD to outperform the ED. The AD's superior performance in high SNR regimes emerges from its amplitude-based decision rule, which becomes increasingly effective as the signal amplitude is more reliably estimated due to the accurate approximation for the nonlinear part of the GLRT results. This result provides valuable references for switching



(a) $SNR = -5$ dB



(b) $SNR = 2$ dB

Figure 6: The probability of error vs. N for the proposed detectors of both simulated and theoretical results.

AD and ED to realize optimal detection.

The influence of the number of samples to P_e is illustrated in Fig. 6, at fixed SNR levels of -5 and 2 dB, isolating the effect of observation length on detection accuracy. In Low SNR case ($SNR = -5$ dB), under severely noise-limited conditions, the ED demonstrates its low SNR optimality. As N increases, P_e steadily decreases for the ED. The AD, although improving with more samples, remains at a higher error probability level than the ED. In High SNR case ($SNR = 2$ dB), AD benefit significantly from larger sample sizes and decreases rapidly as N increases, and always perform better than ED. This behavior validates that the amplitude detector is optimum detector for the high SNR case. (It is noticeable that when SNR is high, the misdetection rate of ED decreases while the false alarm rate is increase to 0.5 , thus the P_e will first decrease when the P_{MD} takes the majority and then increase when the P_{FA} takes lead of the trend of P_e).

The presented probability of error results provide a unified perspective on the detectors' performance across a broad range of operational scenarios. The energy detector excels in low SNR regimes, leveraging energy detection to minimize error rates. Conversely, the amplitude detector demonstrates a pronounced advantage in high SNR conditions, rapidly reducing the probability of error as the number of samples increases and the signal amplitude estimation improves.

V. CONCLUSION

In this paper, we have developed a unified analytical framework for the optimal detection of constant-envelope signals using only the magnitudes of the received samples. By leveraging on the simplified BFED structure, we sidestepped the complexities of traditional IQ-based receivers and phase/frequency synchronization. Through a rigorous Bayesian and GLRT-based analysis, we demonstrated that the optimal detector transitions between two regimes depending on the SNR for the minimum probability of error. In low SNR scenarios, the optimal solution reduces to an energy detector, providing a theoretical foundation for what had previously been a widely used heuristic for the first time. Under high SNR conditions, we derived a novel amplitude detector that uses the MLE of the amplitude to reliably distinguish signals from noise, further simplifying the receiver design. To the best of our knowledge, this is the first time that the optimum signal detector based only on the received signal magnitudes has been derived.

Numerical results confirm the accuracy and robustness of both detectors, validating their theoretical foundations and practical relevance. The closed-form approximations and approximated statistical distributions we introduced enable efficient performance evaluations over a wide range of parameters. Our approach here can be applied in future to the design of simplified receivers for small IoT devices, for spectrum sensing, and so on.

In conclusion, our work not only offers a theoretically optimal and practically implementable detection paradigm but also provides new insights into fundamental relationships between energy detection and amplitude estimation. Further research may explore extensions to the optimal detection in an unknown noise scenario, or to some more general modulation formats.

REFERENCES

- [1] Z. Wei *et al.*, "Integrated sensing and communication signals toward 5g-a and 6g: A survey," *IEEE Internet Things J.*, vol. 10, no. 13, pp. 11 068–11 092, 2023.
- [2] L. Dai, B. Wang, Y. Yuan, S. Han, I. Chih-lin, and Z. Wang, "Non-orthogonal multiple access for 5G: solutions, challenges, opportunities, and future research trends," *IEEE Commun. Mag.*, vol. 53, no. 9, pp. 74–81, 2015.
- [3] Y. Chen, J. Zhang, W. Feng, and M.-S. Alouini, "Radio sensing using 5g signals: Concepts, state of the art, and challenges," *IEEE Internet Things J.*, vol. 9, no. 2, pp. 1037–1052, 2022.
- [4] H. Ye, G. Y. Li, and B.-H. Juang, "Power of deep learning for channel estimation and signal detection in ofdm systems," *IEEE Wirel. Commun. Lett.*, vol. 7, no. 1, pp. 114–117, 2018.
- [5] G. Wang, F. Gao, R. Fan, and C. Tellambura, "Ambient backscatter communication systems: Detection and performance analysis," *IEEE Trans. Commun.*, vol. 64, no. 11, pp. 4836–4846, 2016.
- [6] M. Khani, M. Alizadeh, J. Hoydis, and P. Fleming, "Adaptive neural signal detection for massive mimo," *IEEE Trans. Wirel. Commun.*, vol. 19, no. 8, pp. 5635–5648, 2020.
- [7] S. Yang and L. Hanzo, "Fifty years of mimo detection: The road to large-scale mimos," *IEEE Commun. Surv. Tutor.*, vol. 17, no. 4, pp. 1941–1988, 2015.
- [8] H. He, C.-K. Wen, S. Jin, and G. Y. Li, "Model-driven deep learning for mimo detection," *IEEE Trans. Signal Process.*, vol. 68, pp. 1702–1715, 2020.
- [9] Y. Chen, "Improved energy detector for random signals in gaussian noise," *IEEE Trans. Wirel. Commun.*, vol. 9, no. 2, pp. 558–563, 2010.
- [10] Y. Chen and W. Feng, "Novel signal detectors for ambient backscatter communications in internet of things applications," *IEEE Internet Things J.*, vol. 11, no. 3, pp. 5388–5400, 2024.
- [11] C. Liu, Z. Wei, D. W. K. Ng, J. Yuan, and Y.-C. Liang, "Deep transfer learning for signal detection in ambient backscatter communications," *IEEE Trans. Wirel. Commun.*, vol. 20, no. 3, pp. 1624–1638, 2020.
- [12] R. K. Mallik and R. Murch, "Channel capacity of an asymmetric constellation in rayleigh fading with noncoherent energy detection," *IEEE Trans. Wirel. Commun.*, vol. 20, no. 11, pp. 7375–7388, 2021.
- [13] —, "Suboptimum energy detection receiver using channel norm estimate for simo in rayleigh fading with multi-level ask," *IEEE Trans. Wirel. Commun.*, pp. 1–1, 2024.
- [14] A. Mondal, M. Hanif, and H. H. Nguyen, "SSK-ICS LoRa: A LoRa-Based modulation scheme with constant envelope and enhanced data rate," *IEEE Commun. Lett.*, vol. 26, no. 5, pp. 1185–1189, 2022.
- [15] F. F. Digham, M.-S. Alouini, and M. K. Simon, "On the energy detection of unknown signals over fading channels," *IEEE Trans. Wirel. Commun.*, vol. 55, no. 1, pp. 21–24, 2007.
- [16] S. Zhang, R. Zhang, and T. J. Lim, "Constant envelope precoding for mimo systems," *IEEE Trans. Commun.*, vol. 66, no. 1, pp. 149–162, 2018.
- [17] H. Chougrani, S. Kisseleff, and S. Chatzinotas, "Efficient preamble detection and Time-of-Arrival estimation for Single-Tone frequency hopping random access in NB-IoT," *IEEE Internet Things J.*, vol. 8, no. 9, pp. 7437–7449, 2021.
- [18] N. Yan, H. Zhang, X. Tan, and H. Min, "Analysis and design of a multi-mode wake-up receiver based on direct envelope detection in wireless sensor networks," *IEEE Sens. J.*, vol. 18, no. 22, pp. 9305–9314, 2018.
- [19] Y. Zhang, Y.-C. Liang, and P. Y. Kam, "A Distance-Detection receiver for ambient backscatter communications with MPSK RF source," in *WCNC*, 2020, pp. 1–6.
- [20] K. Witrisal *et al.*, "High-Accuracy localization for assisted living: 5G systems will turn multipath channels from foe to friend," *IEEE Signal Process. Mag.*, vol. 33, no. 2, pp. 59–70, 2016.
- [21] M. Jia, J. Yang, and T. Zhang, "Power allocation in infrastructure limited integration sensing and localization wireless networks," in *VTC2022-Fall*, 2022, pp. 1–5.
- [22] H. Urkowitz, "Energy detection of unknown deterministic signals," *Proc. IEEE*, vol. 55, no. 4, pp. 523–531, 1967.
- [23] P. Y. Kam, S. S. Ng, and T. S. Ng, "Optimum symbol-by-symbol detection of uncoded digital data over the gaussian channel with unknown carrier phase," *IEEE Trans. Commun.*, vol. 42, no. 8, pp. 2543–2552, 1994.
- [24] S. Guruacharya, X. Lu, and E. Hossain, "Optimal non-coherent detector for ambient backscatter communication system," *IEEE Trans. Veh. Technol.*, vol. 69, no. 12, pp. 16 197–16 201, 2020.
- [25] H. L. Van Trees, *Detection, estimation, and modulation theory, part I: detection, estimation, and linear modulation theory*. John Wiley & Sons, 2004, pp. 341–349.
- [26] M.-W. Wu, Y. Jin, Y. Li, T. Song, and P.-Y. Kam, "Maximum-likelihood, magnitude-based, amplitude and noise variance estimation," *IEEE Signal Process. Lett.*, vol. 28, pp. 414–418, 2021.
- [27] Z. Wei, H. Qu, Y. Wang, X. Yuan, H. Wu, Y. Du, K. Han, N. Zhang, and Z. Feng, "Integrated sensing and communication signals toward 5G-A and 6G: A survey," *IEEE Internet Things J.*, vol. 10, no. 13, pp. 11 068–11 092, 2023.
- [28] J. Hu and N. C. Beaulieu, "Accurate simple closed-form approximations to rayleigh sum distributions and densities," *IEEE Commun. Lett.*, vol. 9, no. 2, pp. 109–111, 2005.
- [29] F. D. A. García, H. R. C. Mora, and N. V. O. Garzón, "Novel expressions for rician sum distributions and densities," *IEEE Commun. Lett.*, vol. 25, no. 11, pp. 3513–3517, 2021.